Ray-Tracing Studies for a Whole-Viewing-Angle Retroreflector*

B. Yang and H. Friedsam
Argonne National Laboratory, Argonne, Illinois, USA

1. INTRODUCTION

The APS Survey and Alignment team uses LEICA laser trackers for the majority of their alignment tasks. These instruments utilize several different retroreflectors for tracking the path of the laser interferometer. Currently in use are open-air corner cubes with an acceptance angle of ±20°, corner cube prisms with an acceptance angle of ±50°, and a Cat's eye with an acceptance angle of ±60° (Fig. 1) [1]. Best measurement results can be achieved by using an open-air corner cube that eliminates the need for the laser beam to travel through a different medium before it returns to the instrument detector. However, the trade off is a small acceptance angle.

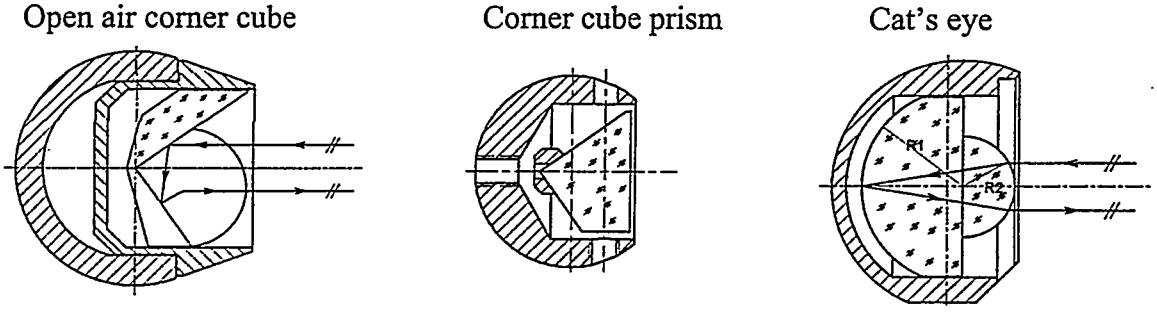

Fig. 1 Corner cube types

In order to overcome the limitations of the small acceptance angles, Takatsuji et al. [2][3] have proposed the creation of a full-viewing-angle retroreflector. Based on the notion that the radius R_1 of a common Cat's eye (Fig. 1) is proportional to R_2, one can write:

$$R_1 = (n-1)R_2 \tag{1.1}$$

In the case that n, the refractive index of glass, equals 2, the radii R_1 and R_2 are identical, and one can create a solid sphere Cat's eye. This design has the advantages that no adhesives are used to bond the two hemispheres together, misalignments between the hemispheres are not an issue, and most importantly, larger acceptance angles are possible. This paper shows the results of our ray tracing calculations characterizing the geometrical optics.

* Work supported by U.S. DOE, Office of Basic Energy Sciences, under Contract No. W-31-109-ENG-38.

DISCLAIMER

DISCLAIMER

Portions of this document may be illegible in electronic image products. Images are produced from the best available original document.

2. CALCULATIONS AND RESULTS

2.1 Single Ray-Tracing Calculations

For the purpose of this exercise the origin of the coordinate system is located at the center of the Cat's eye with radius R and refractive index n. The light ray bundle is symmetric to the z-axis pointing counter parallel to the incoming rays. Every incident ray can be represented by its impact parameter b, which can be expressed as

$$b = R\sin(\phi). \tag{2.1}$$

Due to the cylindrical symmetry, the intensity distribution of the beam can be represented as a function f(b) depending only on the radial coordinate b (Fig. 2).

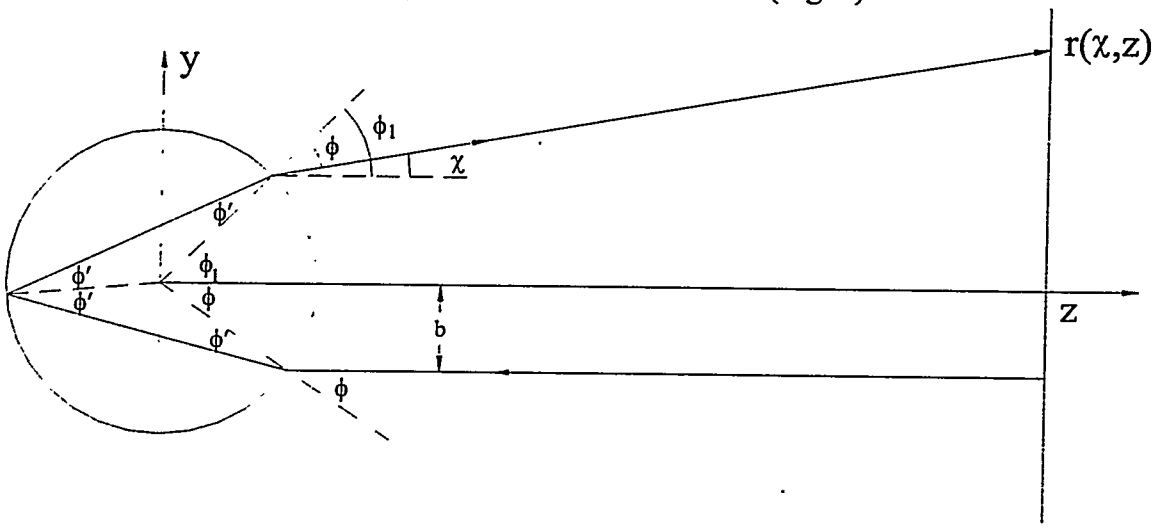

Fig. 2 Ray-tracing schematic for a retroreflecting sphere

From the law of reflection one can ascertain that the inner angles ϕ' of the small triangles at the circle perimeter are identical because each triangle has two sides equal to the radius R of the sphere. Thus

$$\phi + \phi_1 = 4\phi' \quad \text{and} \quad \chi = \phi_1 - \phi. \tag{2.2}$$

The law of refraction on the other hand dictates that

$$\sin(\phi) = n\sin(\phi'). \tag{2.3}$$

Using this information, one can derive the formula for the deflection angle χ to be

$$\chi = 4\sin^{-1}\left(\frac{\sin\phi}{n}\right) - 2\phi. \tag{2.4}$$

At a distance z from the origin the transverse coordinate of the reflected ray is given by

$$r(\chi, z) \cong R\sin(\phi + \chi) + z\sin\chi, \tag{2.5}$$

taking into account the fact that $z >> R$. This transfer function maps the transverse coordinate of an incident ray to that of the corresponding reflected ray. It can be approximated by a Taylor series expansion

$$\chi \cong \frac{2\phi}{n}\left(2-n-\frac{\phi^2}{4}\right). \tag{2.6}$$

Using this approximation, the maximum deflection angle χ_m is

$$\chi_m = 4\left(\frac{2-n}{3}\right)^{\frac{3}{2}} \text{ for } \phi_m = 2\sqrt{\frac{2-n}{3}}. \tag{2.7}$$

The exact back reflection occurs for $\chi = 0$ when

$$\phi = \phi_0 \equiv 2\sqrt{2-n} = \sqrt{3}\phi_m. \tag{2.8}$$

Equation (2.6) can now be written as

$$\chi \cong -\frac{\phi}{2n}\left(\phi^2-\phi_0^2\right) \cong -\frac{\phi}{4}\left(\phi^2-\phi_0^2\right), \quad \text{with n} \approx 2. \tag{2.9}$$

On the other hand, the intensity distribution of the reflected beam is inversely proportional to the illuminated areas. Therefore one can equate

$$F(r,z) = f[b(r)]\frac{bdb}{rdr} \approx f[R\sin\phi]\frac{R^2\sin 2\phi}{z\dfrac{d}{d\phi}\left[R\sin(\phi+\chi)+z\sin\chi\right]^2}, \tag{2.10}$$

where F(r,z) is the intensity distribution of the reflected beam and f[$b(r)$] is the intensity distribution of the input beam. For simplicity of the following derivations we assumed a constant intensity profile of the input beam and not a Gaussian distribution. For incident rays near the angle of maximum positive deflection,

$$\frac{dr}{db} = \frac{R\cos(\phi+\chi)\left(1+\dfrac{d\chi}{d\phi}\right)+z\cos\chi\dfrac{d\chi}{d\phi}}{R\cos\phi} = 0, \tag{2.11}$$

the intensity distribution F(r, z) approaches infinity. This leads to the condition

$$\frac{d\chi}{d\phi} = \frac{R\cos(\phi+\chi)}{z\cos\chi+R\cos(\phi+\chi)} \approx 0, \qquad (z << R). \tag{2.12}$$

In order to understand how this occurs, the relationship between ϕ and χ, as expressed in Equation (2.4), is plotted in Fig. 3 for refractive indices above and below n = 2. The curves in this figure are (A) for a refractive index n = 1.98, (B) n = 2.00, and (C) n = 2.02.

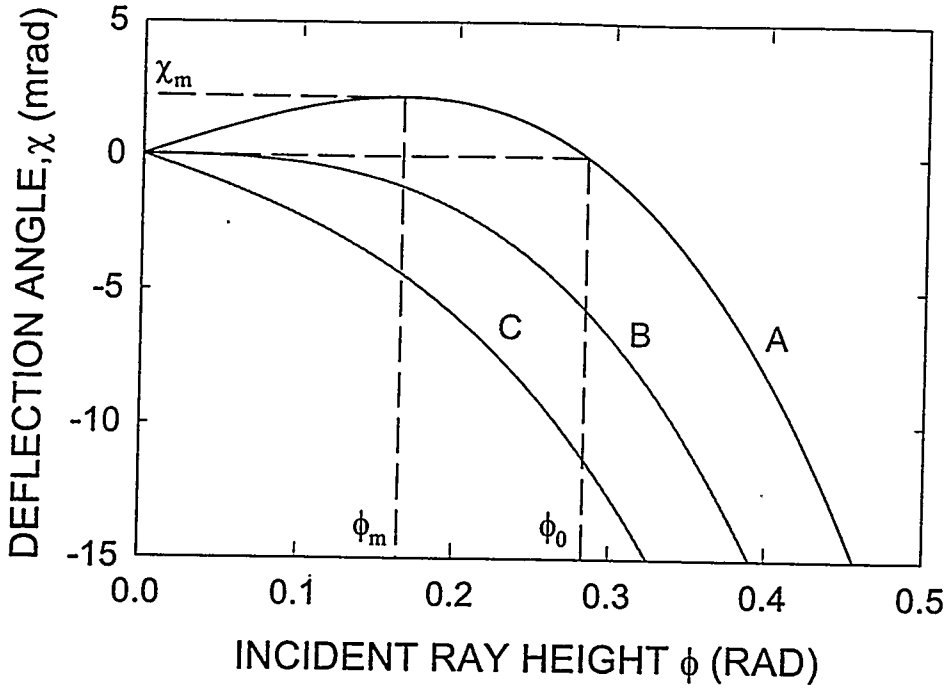

Fig. 3 Transfer function for incident and reflected rays of different refractive indices n [(A) n=1.98, (B) n=2.00, and (C) n=2.02]

- One can observe that the on-axis incident ray ($\phi = 0$) is reflected back on axis ($\chi = 0$).
- For $n > 2.00$ all rays are "over bent," leading to negative reflection angles χ for all incident ray heights. The reflected rays are not focused but spread out.
- For $n < 2.00$, only rays far away from the optical axis ($\phi > \phi_0$) are "over bent." In the vicinity of the zero incidence angle, the reflected angle increases until it reaches a maximum deflection angle χ_m. Near the maximum ($\phi \sim \phi_m$), all incident rays are mapped into a very narrow range of reflection angles ($\chi \sim \chi_m$). These reflected rays near the maximum angle χ_m lead to a well-defined annular light cone.
- The case $n = 2.00$ can be viewed as a special case for $n < 2.00$, when the maximum deflection occurs on-axis at $\phi_m = 0$, and the "cone" has a zero opening angle.

2.2 Vertex and Opening Angle of the Light Cone

From the preceding discussion, one can see that the focusing for n < 2.00 plays the central role in allowing reflected rays to form a tight ray bundle. Its properties need to be studied carefully.

First, the formation of the light cone is unique. It is not formed by Gaussian optics, where the transfer function from the incident height ϕ to the exit angle χ is linear. Instead, the Cat's eye focuses through a singularity in the derivative of the transfer function.

While a Gaussian optical system often produces a light beam with a focal point in real space, the Cat's eye produces a ring in the momentum space, or an annular light cone in real space. The virtual vertex of the cone is located at

$$z = -\frac{R\sin\phi_m}{\sin\chi_m}. \tag{2.13}$$

The maximum reflection angle χ_m can be obtained from the derivative of Equation (2.4):

$$\chi_m = 4\sin^{-1}\left(\frac{\sin\phi_m}{n}\right) - 2\phi_m = 2\sin^{-1}\left[\frac{1}{n^2}\left(\frac{4-n^2}{3}\right)^{\frac{3}{2}}\right]. \tag{2.14}$$

The light cone angle is determined solely by the index of refraction and is independent of the geometric dimensions of the sphere. Figure 4 shows the dependence of the light cone angle on the refractive index where χ_m is depicted on a log scale. In order to use a glass sphere as a retroreflector, a small opening angle of the light cone is required. For example, if we wish to keep the diameter of the reflected light cone less than 20 mm at 10 m from the reflector, the opening angle should satisfy

$$\chi_m < \frac{10\ mm}{10\ m} = 1.0\ (mrad). \tag{2.15}$$

In this case the refractive index of the glass should be in the range $1.988 < n < 2.000$.

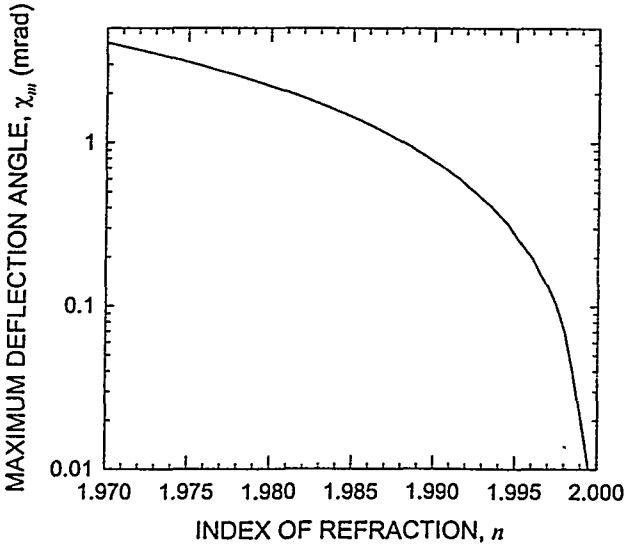

Fig. 4 Maximum deflection angle of the Cat's eye, as a function of n

2.3 Efficiency of the Whole-Viewing-Angle Retroreflector

Undesirable reflections and transmissions from the sphere surfaces and the divergence of the beam diminish the light intensity of the reflected light. The total efficiency η due to the transmission and reflection losses η_{R_i} at the three surface boundaries between the glass sphere and air is

$$\eta = \eta_{R1} \cdot (1 - \eta_{R2}) \cdot \eta_{R3} . \tag{2.16}$$

For a whole viewing angle reflector, all surfaces are identical and hence

$$\eta = \eta_R{}^2 (1 - \eta_R) . \tag{2.17}$$

If the coating of the glass surface is designed appropriately to maximize the total efficiency, then

$$\eta_{\max} = \frac{4}{27} \text{ when } \eta_R = \frac{2}{3} . \tag{2.18}$$

This means that by using this reflector, about 85% of the incoming light intensity is lost due to the reflections and transmissions at the sphere surfaces. This is a very poor efficiency factor that can only be overcome by increasing the beam intensity. However, by limiting the acceptance angle to about 180° and mirror coating one half of the sphere, one can gain almost 100% efficiency.

For analyzing the effects of the diverging beam, we assume that the incoming laser beam has a uniform intensity within its radius ($b < \rho$), and the detector can make use of the reflected beam within a limited divergence angle δ. In order to contain all of the reflected light within the usable solid angle, the divergence angle δ has to be equal or larger than the reflected ray angle χ:

$$\delta > \chi = 4 \sin^{-1}\left(\frac{\sin\phi}{n}\right) - 2\phi , \text{ for } 0 < \phi < \sin^{-1}\left(\frac{\rho}{R}\right) . \tag{2.19}$$

One way to satisfy this condition is to use a large sphere. However, in order to optimize the design, we want to know the minimum usable sphere size. Figure 5 illustrates the conditions for selecting the minimum sphere.

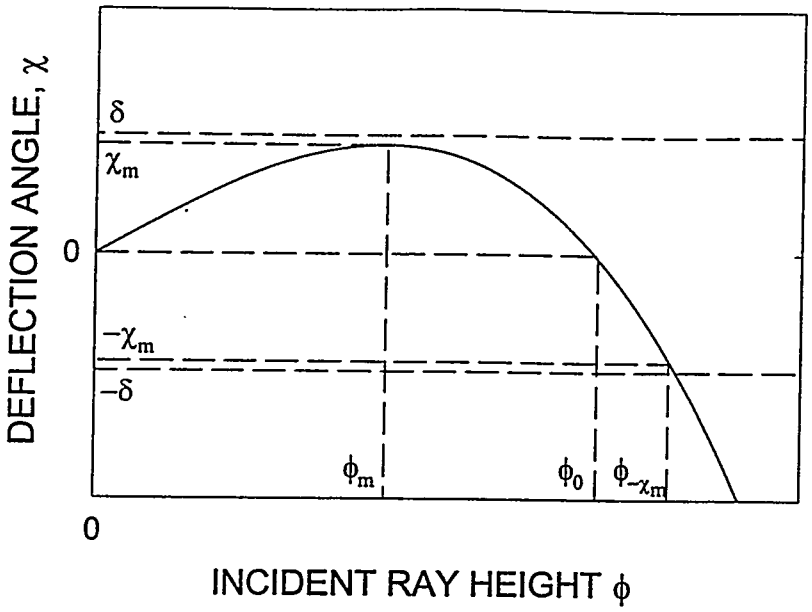

Fig. 5 Illustration of the conditions for calculating the minimum sphere radius

Two steps are required to solve this problem. In the first step the material of the reflector has to be chosen such that the maximum deflection angle is within the acceptance window of the detector. The detector acceptance window is shown in Fig. 5 by the region $-\delta \le \chi \le \delta$ and the material of the reflector is chosen such that $\chi_m < \delta$. Using Equation (2.7), it follows that

$$\delta \ge \chi_m = 4\left(\frac{2-n}{3}\right)^{\frac{3}{2}}, \tag{2.20}$$

or, when solved for the refractive index n,

$$n \ge 2 - 1.19 \cdot \delta^{\frac{2}{3}}. \tag{2.21}$$

In the second step we chose the radius of the sphere such that all incident rays fall within the window with a radius of $\rho \cong R\phi_{-\delta}$. Using the approximation provided in Equation (2.9), one can derive the value of $\phi_{-\delta}$ as

$$-\delta \cong \frac{\phi_{-\delta}}{4}\left(\phi_0^{\,2} - \phi_{-\delta}^{\,2}\right). \tag{2.22}$$

If we use Equation (2.20) to relax (2.22), we obtain

$$-\chi_m \cong \frac{\phi_{-\chi_m}}{4}\left(\phi_0^{\,2} - \phi_{-\chi_m}^{\,2}\right). \tag{2.23}$$

With that, the following simple solution can be obtained:

$$\phi_{-\chi_m} = 2\phi_m = \frac{2}{\sqrt{3}}\phi_0 . \tag{2.24}$$

Hence, the radius of the acceptance aperture for the incidence laser beam is given by

$$\rho_{-\chi_m} = R\phi_{-\chi_m} = \frac{2R}{\sqrt{3}}\phi_0 . \tag{2.25}$$

3. DESIGN STUDY FOR A CAT'S EYE

In this section, we apply the results from the theoretical derivations to design a Cat's eye and use the ray tracing program ZEMAX [4] to verify the conclusions of the analytical studies.

The following conditions for our design are assumed:

1. The incident laser beam radius $b_{\max}$ is 4 mm.
2. The reflected beam should have an opening angle of less than 0.2 mrad.

Using Equation (2.21) with $\delta = 0.2 \times 10^{-3}$, we obtain the constrain on the material of the Cat's eye:

$$2.00 > n \geq 2 - 1.19 \cdot \delta^{\frac{2}{3}} = 1.9959. \tag{3.1}$$

We found that O'HARA [5] glass type LAH79 satisfies this requirement with

$$n = 1.99613 \text{ at } \lambda = 632.8 \text{ (nm)}. \tag{3.2}$$

For this glass, the light cone angle is given by Equation (2.20)

$$\chi_m = 4\left(\frac{2-n}{3}\right)^{\frac{3}{2}} = 0.186 \text{ (mrad)}, \tag{3.3}$$

and the approximate acceptance angle is given by Equation (2.24)

$$\phi_{-\chi_m} = 4\sqrt{\frac{2-n}{3}} = 0.144 \text{ (rad)}. \tag{3.4}$$

Applying Equation (2.25), the minimum radius of the sphere satisfying the first condition can be is obtained:

$$R = \frac{\rho}{\phi_{\chi_m}} = \frac{4 \text{ (mm)}}{0.144} = 28 \text{ (mm)}. \tag{3.5}$$

In order to validate the chosen parameters and verify the analytical calculations in the previous section, we used ZEMAX to perform ray tracing calculations for various glass spheres with radii R = 12.5 mm, 20 mm, and 40 mm. The incident beam is represented by a bundle of parallel rays packed randomly in a cylinder with a 4-mm radius.

Case 1: Sphere radius $R = 20$ mm

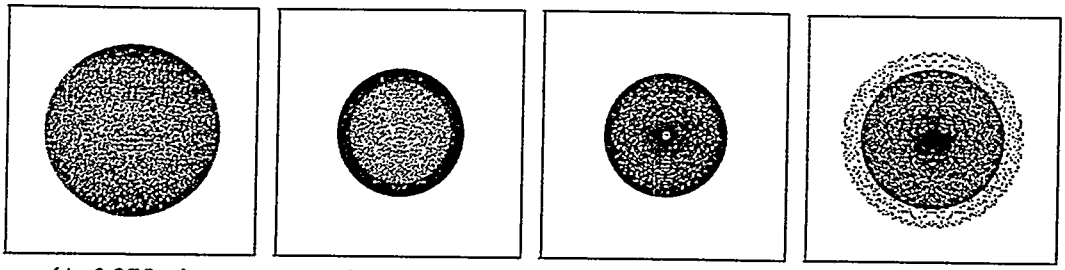

(A: 0.375 m) (B: 1.5 m) (C: 3.0 m) (D: 6.0 m)

Fig. 6 Ray tracing spot diagrams for O'HARA glass sphere type LAH79 with a diameter of 40 mm and an incident beam with a diameter of 8 mm. Each box is a 10 mm × 10 mm square.

Figure 6 shows the spot diagrams for a 20-mm-radius sphere, with screen locations at 0.375 m, 1.5 m, 3.0 m, and 6.0 m from the sphere, respectively. At very short distances from the sphere, the reflected ray coordinates are dominated by the initial displacement, essentially the first term of Equation (3.6), and the beam distribution is a good approximation of the incident beam. As the light propagates away from the sphere, the reflection angle becomes important. At 1.5 m from the source, an annular structure can be clearly seen. While the outer diameter of the ring is given approximately by

$$\rho_{outer} = R\sin\phi_m + z\sin\chi_m, \tag{3.6}$$

the over-bent marginal rays give the inner diameter, via Equation (2.5), as

$$\rho_{inner} = R\sin\phi_{\max} + z\sin\chi(\phi_{\max}). \tag{3.7}$$

Due to the negative deflection angle, the marginal rays close in on the optical axis near z = 3.0 m. At the distance of 6 m, the marginal rays overshoot the boundary of the light cone.

Case 2: Sphere radius $R = 40$ mm

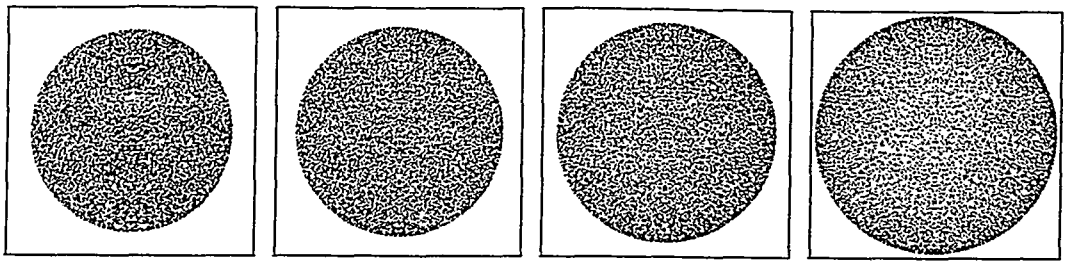

(A: 0.375 m) (B: 1.5 m) (C: 3.0 m) (D: 6.0 m)

Fig. 7 Ray tracing spot diagrams for O'HARA glass sphere type LAH79 with a diameter of 80 mm and an incident beam with a diameter of 8 mm. Each box is a 10 mm × 10 mm square.

Figure 7 shows the spot diagrams for the sphere with a 40-mm radius, using the same spacing for the screen locations. The sphere is slightly larger than the minimum required radius of 28 mm as calculated by Equation (3.5). In this case the beam is entirely enclosed in the acceptance window, and therefore all reflected rays are contained within the light cone. One can see that the spot increases with distance at the rate of the opening angle calculated in Equation (3.3).

Case 3: Sphere radius $R = 12.5$ mm

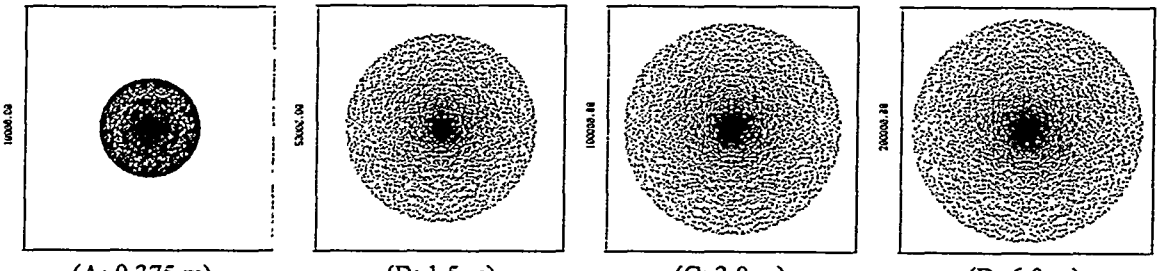

(A: 0.375 m) (B: 1.5 m) (C: 3.0 m) (D: 6.0 m)

Fig. 8 Ray tracing spot diagrams for O'HARA glass sphere type LAH79 with a diameter of 25 mm and an incident beam with a diameter of 8 mm. In this case each box shows a different size.

Figure 8 shows the spot diagram for a sphere with a 12.5-mm radius, also with the screen located at 0.375, 1.5, 3.0, and 6.0 m from the sphere, respectively. In this case a large portion of the beam is beyond the acceptance window, and the reflected beam expands rapidly at large distances so that different box sizes were necessary to show the results. At 0.375 m the box size is 10 mm square, at 1.5 m it is 50 mm square, at 3.0 m it is 100 mm square, and at 6 m a box size of 200 mm is required. However, when zooming in on the center of the spot, the central feature of an annular light ring is still detectable. This design implies a reduction in the intensity of the center of the reflected beam.

4. DISCUSSION OF THE RESULTS

Previous studies determined the ideal refractive index (n) to be 2.0 for a whole-viewing-angle Cat's eye. In contrast, we found in this work that the formation of a light cone for $n < 2.00$ is particularly important for the application of this type of reflector. The annular light cone is formed by a singularity in the derivative of the transfer function of the reflector. Its opening angle depends only on the refractive index of the sphere.

The numerical ray tracing has verified several major conclusions from the preceding sections:

(1) We did find the existence of an annular light cone with a sharp boundary as predicted by theory through the ray tracing results.

(2) The acceptance aperture defined by $\frac{2R}{\sqrt{3}}\phi_0$ is a quantitative measure for predicting the performance of the Cat's eye. When the beam is smaller than or comparable to the acceptance aperture, the light rays are well contained in the cone. When the beam is significantly larger than the acceptance aperture, the reflected light rays rapidly diverge.

(3) The optical material with $n = 2.00$ is not optimized in its acceptance aperture. It is better to use material with $n < 2.0$. The optimal index of refraction is $n = 2 - 1.19 \cdot \delta^{2/3}$, for a given beam divergence δ.

Future studies are planned and some modifications are expected. Efficiency calculations based on a realistic beam intensity distribution such as a Gaussian beam profile is expected to provide a better estimate in the form of a continuous function. It will also replace the approximation for the acceptance aperture. Furthermore, a wave optics calculation of the intensity of the reflected light is expected to remove the singularity near the cone boundary. Finally, it would be desirable to perform a comparison with respect to the existing Cat's eye design shown in Figure 1.

5. CONCLUSION

In Section 2 we derived the analytical expressions for choosing the index of refraction n of a glass sphere based on the specifications of the reflected beam. We also provided an approximation for calculating the minimum radius of a reflector sphere based on efficiency considerations. Finally, in section 3, the analytically derived results were confirmed in a design study for a Cat's eye.

The major result of this analysis is the discovery that a Cat's eye, unlike Gaussian optics, focuses through a singularity in the derivative of the transfer function, producing an annular light cone. Utilizing a sufficiently large sphere radius, this property can be used to design a whole-viewing-angle retroreflector. However, as shown in section 2.3, the intensity efficiency of this design is less than optimal.

6. REFERENCES

[1] LEICA LT500/LTD500 3D-Laser Tracking System – The Hardware.

[2] Toshiyuki Takatsuji, Mitsuo Goto, Sonko Osawa, Ruimin Yin, Tomiz Kurosawa, *Whole viewing angle cat's eye retroreflector as a target for laser trackers*, Measurement Science and Technology, 10, pp. N87-N90, 1999.

[3] Toshiyuki Takatsuji, Yoshihisa Tanimura, Sonko Osawa, Tomiz Kurosawa, *Laser Tracking Coordinate System Developed by NRLM*, paper presented at the International Dimensional Metrology Workshop, Knoxville, TN, 1999.

[4] Focus Software, Incorporated, ZEMAX 6.0.

[5] O'HARA Optical Glass (Glass Catalog Overseas Version).